ELSEVIER

Ceramics International 31 (2005) 121–127

CERAMICS INTERNATIONAL

www.elsevier.com/locate/ceramint

Investigation of parameters affecting grain growth of sintered magnesite refractories

Cemail Aksel[a,*], Ferit Kasap[b,1], Ali Sesver[c]

[a]*Department of Materials Science and Engineering, Anadolu University, Iki Eylül Campus, Eskisehir 26470, Turkey*
[b]*TÜBİTAK Ceramic Research Centre, Anadolu University, Iki Eylül Campus, Eskisehir 26470, Turkey*
[c]*KÜMAŞ, Kütahya Magnesite Corporation, Kütahya 43001, Turkey*

Received 13 January 2004; received in revised form 30 March 2004; accepted 30 March 2004
Available online 15 July 2004

Abstract

The parameters influencing grain size of sintered magnesite such as temperature (1700 and 1800 °C), time (19 and 50 min), cooling rate (5, 10 and 25 °C min^{-1}) and various particle size (−3; +3,−5; +5,−8; +8,−10 mm) were investigated using different sintering regimes to improve grain growth. The effects of impurities (i.e. SiO_2, CaO, Fe_2O_3, and CaO/SiO_2 ratio) on grain growth were also evaluated by EDX analysis for each sample based on the variation of particle size, cooling rate and the change in the colour of samples (dark–light). For the samples sintered at 1700 °C, the decrease in the cooling rate from 10 to 5 °C min^{-1} and the increase in the dwell time from 19 to 50 min enhanced grain size significantly. The rise in sintering temperature to 1800 °C for 19 min, using cooling rate of 25 °C min^{-1}, resulted in maximum grain growth (~140 μm) for +3,−5 mm particle size of dark-coloured samples.

Keywords: A. Sintering; B. Grain size; D. MgO; E. Refractory

1. Introduction

Grain size and boundaries, impurities and/or additives, porosity, sintering temperature and shaping practice play an important role in controlling many physical, mechanical and chemical properties of magnesia-based bricks [1–8]. It is known [2,3] that porosity can alter or eliminate the appearance of grain-size control of strength. As grains grow, grain boundaries sweep past many pores, which are then within the grains not at grain boundaries. This generally results in a more regular pore shape, which may reduce stress concentrations. It is also stated [3,4] that impurities and/or additives within the grains have quite different effects on strength, depending on the mechanism of failure. With increasing additive content and increasing grain size, which results in a decline in grain-boundary area, many grain boundaries become covered with precipitates. At low temperatures, solution or precipitates within the grains normally cannot make significant changes in the elastic modulus or fracture energy and thus in the stress to cause flaw failure. As the temperature increases, some oxide impurities, especially SiO_2, start to soften and enhance grain-boundary sliding. The increasing concentration of impurities at grain boundaries is therefore the cause of the lower relative strengths at large grain sizes. The latest researchers [5–8] reported that the amount of additive and its size are the major parameters affecting mechanical and thermal properties of magnesia-based materials, and the variation in magnesia grain size is also a contributing factor influencing strength.

The size of the MgO crystals within the magnesia grains is critically an important factor in controlling the resistance to corrosive attack of basic bricks [9]. When the size of the crystals increases, a corresponding decline occurs in crystal surface area and open porosity, which makes the grains less reactive for infiltrating iron oxide rich slag in MgO-based refractories [10]. Furthermore, as the mean MgO grain size

* Corresponding author. Tel.: +90 222 3350580x6355; fax: +90 222 3239501.
E-mail address: caksel@anadolu.edu.tr (C. Aksel).
[1] Present address: Plant, Medicine and Scientific Research Centre, Anadolu University, Yunusemre Campus, Eskisehir 26470, Turkey.

0272-8842/$30.00 © 2004 Elsevier Ltd and Techna S.r.l. All rights reserved.
doi:10.1016/j.ceramint.2004.03.046

increases, the wear rate as a result of corrosive slag attack decreases [10]. Magnesia-based refractories with a large grain size (>100 μm) are used extensively where the corrosion resistance is required. In contrast, a high thermal shock resistance in fused magnesia grain requires a fine crystal size and a compromise may be required in applications where thermal shock resistance is important [11].

Critical microstructural factors affecting properties and performance of a brick are basically grain size, impurities and CaO/SiO_2 ratios [9]. A standard brick contains varying amounts of impurity arising from the raw materials or added deliberately such as SiO_2, Al_2O_3, Fe_2O_3, FeO and CaO that provide a silicate bonding phase. As the CaO/SiO_2 ratio is ~1, a significant amount of liquid forms at relatively low temperature in the bond between the magnesia clinker as a consequence of the low melting point (T_m = 1495 °C) of the $CaO{\cdot}MgO{\cdot}SiO_2$ composition, leading to a decrease in refractoriness [9,12,13]. The microstructure of a brick with CaO/SiO_2 ratio about 2 contains generally more refractory crystal phases such as $2CaO{\cdot}SiO_2$ (T_m = 2130 °C) and $3CaO{\cdot}MgO{\cdot}2SiO_2$ (T_m = 1575 °C) at grain boundaries on cooling [9,12,13]. The further increase in the CaO/SiO_2 ratio ($\gg 2$) results in abrasion, infiltration and a decline in refractoriness [13]. In general, a high amount of CaO causes destruction and fracture of the lining during firing due to the formation of low melting point calcium aluminate [14]. Furthermore, a large amount of silicate in the brick leads to a decline in the resistance to spalling and refractoriness [15]. During firing at the outlet of sintering zone, Fe_2O_3 is also converted to FeO with a dramatic reduction in volume, leading to spalling and destruction of the brick [14,16]. A magnesia-based brick refractory for the cement industry should therefore have as little Fe_2O_3 as possible (<1%) [13]. A significant amount of Al_2O_3 can also bring about an improvement in thermal shock resistance of the brick, but decreases refractoriness and causes spalling [13]. This is because mayenite ($12CaO{\cdot}7Al_2O_3$) is formed by a reaction with CaO from the kiln feed due to overheating, and thus the Al_2O_3 content should be sufficient for elastification of the brick, but as low as possible [13]. In general, using the highest quality raw materials, resulting in the optimum MgO and Al_2O_3 content, the minimised Fe_2O_3 and the optimum CaO/SiO_2 ratio prevent the formation of low-melting compounds with brick and kiln feed components. The raw materials for the individual brick grades are therefore carefully selected so that the different bricks are able to cope in the best possible way with the conditions prevailing in the corresponding zones of rotary cement kilns.

Nowadays, one of the current research areas focused on the improvement in the resistance of corrosive attack of sintered magnesite with the greatest grain growth. As the grain size increases, the penetration of slag through the grain boundaries can be minimised. So that wear rate and weight loss can be inhibited. The development in grain size leads to a high resistance to fracture and erosion. To reach the optimum grain size increases the quality and performance of the refractory material, leading to an economical benefit and longer service life for industrial applications in terms of corrosion and thermal shock resistance. In this work, the effects of parameters (i.e. temperature, time, cooling rate, different particle size and the change in the colour of samples) on grain growth of sintered magnesites were investigated using different sintering regimes, and the reasons for this are examined. The roles of existing impurities (i.e. SiO_2, CaO, Fe_2O_3, and CaO/SiO_2 ratio) on the enlargement of grain size were also evaluated by EDX analysis. It is considered that this paper will provide a platform to improve understanding of relationships between microstructure and those parameters, affecting grain size of the sintered magnesite significantly.

2. Experimental procedure

Raw material magnesite was classified into four groups, as a range of (in mm): (i) (−3), (ii) (+3,−5), (iii) (+5,−8) and

Table 1
EDX analysis and MgO mean grain size of sintered magnesite for a range of particle size, using different cooling rates (T_s = 1700 °C and t_{dwell} = 19 min)

Samples	Particle size (mm)	Mean grain size (μm)	EDX analysis (%)					CaO/SiO_2	Cooling rate (°C min^{-1})
			MgO	Al_2O_3	SiO_2	CaO	Fe_2O_3		
Light	(−3)	29.6	97.77	0.93	0.74	0.34	0.22	0.46	5
Dark	(−3)	34.3	95.28	0.38	2.39	0.51	1.44	0.21	5
Light	(+3,−5)	32.9	96.59	2.02	0.17	1.17	0.06	6.88	5
Dark	(+3,−5)	36.9	97.48	0.19	0.59	1.26	0.48	2.14	5
Light	(+5,−8)	33.7	96.60	0.77	2.19	0.54	0.10	0.25	5
Dark	(+5,−8)	44.0	94.71	1.23	1.21	0.83	2.03	0.69	5
Light	(+8,−10)	29.0	97.34	0.55	0.50	1.33	0.28	2.66	5
Dark	(+8,−10)	32.4	97.40	0.20	0.56	0.98	0.87	1.75	5
Light	(−3)	25.0	98.21	0.16	0.53	0.84	0.27	1.58	10
Dark	(−3)	37.8	97.30	0.30	0.80	0.12	1.49	0.15	10
Light	(+3,−5)	29.7	96.61	1.52	0.60	1.16	0.12	1.93	10
Dark	(+3,−5)	31.6	94.94	0.92	2.33	0.45	1.35	0.19	10
Light	(+5,−8)	11.5	97.22	1.19	0.47	1.13	0.02	2.40	10
Dark	(+5,−8)	30.9	96.93	0.84	0.58	0.66	0.99	1.14	10
Light	(+8,−10)	15.8	97.84	0.11	0.24	1.48	0.33	6.17	10
Dark	(+8,−10)	30.9	97.04	0.57	1.28	0.54	0.57	0.42	10

Table 2
EDX analysis and MgO mean grain size of sintered magnesite for a range of particle size, using different cooling rates (T_s = 1700 °C and t_{dwell} = 50 min)

Samples	Particle size (mm)	Mean grain size (μm)	EDX analysis (%)					CaO/SiO_2	Cooling rate (°C min^{-1})
			MgO	Al_2O_3	SiO_2	CaO	Fe_2O_3		
Light	(−3)	41.8	98.76	0.13	0.36	0.66	0.10	1.83	5
Dark	(−3)	44.2	96.49	0.47	1.73	0.43	0.88	0.25	5
Light	(+3,−5)	35.5	97.96	0.18	0.57	1.22	0.07	2.14	5
Dark	(+3,−5)	37.8	97.69	0.14	1.29	0.77	0.10	0.60	5
Light	(+5,−8)	37.1	98.22	0.02	0.61	1.14	0.05	1.87	5
Dark	(+5,−8)	42.6	91.06	0.24	6.39	1.12	1.18	0.18	5
Light	(+8,−10)	46.6	87.04	0.23	11.04	1.15	0.54	0.10	5
Dark	(+8,−10)	49.2	97.80	0.01	0.35	1.65	0.20	4.71	5
Light	(−3)	29.3	98.63	0.44	0.34	0.25	0.34	0.74	10
Dark	(−3)	30.1	98.52	0.22	0.40	0.17	0.70	0.43	10
Light	(+3,−5)	36.4	97.64	0.40	1.20	0.51	0.21	0.43	10
Dark	(+3,−5)	36.8	94.13	0.49	2.41	0.42	2.53	0.17	10
Light	(+5,−8)	34.2	97.26	0.26	1.05	1.05	0.38	1.00	10
Dark	(+5,−8)	41.3	97.01	0.50	0.89	0.80	0.80	0.90	10
Light	(+8,−10)	46.2	96.78	0.17	0.48	2.32	0.25	4.83	10
Dark	(+8,−10)	48.2	96.50	0.23	1.37	1.06	0.85	0.77	10

(iv) (+8,−10) particle size. A sintering procedure similar to industrial conditions was carried out at 1700 °C for 19 min using cooling rates of 5 and 10 °C min^{-1} for each particle range. The soaking time was then increased to 50 min using the same sintering route to observe the effect of dwell time on grain growth of magnesites. Furthermore, two types of magnesite (samples A and B) with a different chemical composition were sintered at 1800 °C for 19 min, where the cooling rate was 25 °C min^{-1}. The chemical composition of each sintered sample as a function of particle size using EDX analysis was given in Tables 1–3. After sintering, samples were in general categorised into two groups in terms of colour change (e.g. dark or light colour samples). The effects of impurities leading to colour change, cooling rate and particle size on the development of grain size were then examined for each sample. Then, bulk density values were measured using the standard water immersion method [17]. Samples were placed in polyethylene moulds using a mixture of epoxy resin and hardener. Surfaces of samples were ground using progressively finer SiC papers. The polishing of specimens for SEM-EDX examination was carried out using a 1 μm diamond spray at the final stage in a ''Planopol/Pedemax'' automatic polishing machine. Chemical etching was then carried out in a HNO_3 and distilled water (1:1) solution at room temperature for ~5 min [18]. After gold coating, microstructural examination of the relevant samples was carried out using a CamScan-S4 Scanning Electron Microscopy (SEM).

Grain sizes of polished and chemically etched surfaces were then measured from photographs taken in SEM, using a

Table 3
EDX analysis and MgO mean grain size of sintered magnesite for a range of particle size (T_s = 1800 °C, t_{dwell} = 19 min and cooling rate = 25 °C min^{-1})

Samples	Particle size (mm)	Mean grain size (μm)	EDX analysis (%)				
			MgO	Al_2O_3	SiO_2	CaO	Fe_2O_3
Sample A							
Light	(−3)	98.8	96.20	2.33	0.07	0.85	0.69
Dark	(−3)	74.3	97.67	0.27	0.77	1.23	0.05
Light	(+3,−5)	99.8	97.11	0.60	1.02	0.86	0.40
Dark	(+3,−5)	138.8	95.64	1.27	1.50	1.24	0.34
Light	(+5,−8)	64.0	97.35	0.06	0.91	1.20	0.60
Dark	(+5,−8)	91.9	96.10	0.29	1.50	1.39	0.72
Light	(+8,−10)	100.0	98.03	0.15	0.48	1.09	0.25
Dark	(+8,−10)	123.4	96.99	0.20	0.85	1.73	0.22
Sample B							
Light	(−3)	40.1	98.24	0.07	0.43	0.68	0.57
Dark	(−3)	59.8	98.54	0.04	0.72	0.23	0.47
Light	(+3,−5)	33.7	97.94	0.06	0.49	0.68	0.90
Dark	(+3,−5)	34.3	97.47	0.24	0.83	0.96	0.51
Light	(+5,−8)	37.6	97.85	0.03	1.03	0.82	0.26
Dark	(+5,−8)	60.4	97.20	0.09	1.08	0.46	1.17
Light	(+8,−10)	57.0	97.54	0.30	0.97	1.12	0.08
Dark	(+8,−10)	61.5	97.41	0.21	1.02	0.79	0.56

standard line mean intercept method [19]. Average grain size was determined from intercept measurements on the observed plane, by using the following:

$$\overline{D} = 1.56\overline{L} \quad (1)$$

where $\overline{D}$ is the average grain size and $\overline{L}$ is the average intercept length, taken over a large number of grains and measured on the plane of polish. Assumptions for the grain size variables, made in order to specify an average grain size, were that the structure consisted of nontextured, equiaxed grains of regular polyhedral shape. All the values calculated for each sample were the average value of ~100 measurements of three SEM micrographs. According to those values, the improvement in grain growth was investigated for each sample based on the effect of impurities, colour change, cooling rate, temperature, time and particle size.

3. Results and discussion

Fig. 1 shows mean grain size of sintered magnesite for a range of particle sizes, using different cooling rates from the production temperature of 1700 °C, where the dwell time was 19 min. There was a significant fluctuation in grain size as a function of particle size. The observed trend in general indicates that the grain size of sintered magnesite using a low cooling rate increased with increasing particle size apart from the coarsest one; however, samples with a high cooling rate exhibited a marked decline in grain size as a function of rising particle size. Figs. 2 and 3 demonstrated the greatest and smallest mean grain size for the range of +5,−8 mm particle size, respectively. This variation was as a consequence of the decline in the cooling rate from 10 to 5 °C min^{-1}, which caused an increase in the grain size by a factor of ~4. The lower the cooling rate, the larger the grain growth was obtained using this sintering regime. Sintered materials with darker colour were in general illustrated a marked improvement in grain size, as compared to materials with lighter colour (Fig. 1 and Table 1). EDX analysis given in Table 1 showed that the reason for the change to the dark colour is the presence of a considerable amount of Fe_2O_3 (≤2%). CaO content in light-coloured materials using faster cooling rate was also higher than that of dark samples; however, use of lower cooling rate reduced the amount of CaO significantly in the light-coloured samples. In general, the amount of SiO_2 was higher, and CaO/SiO_2 ratios were smaller for the dark-coloured samples than those of light-coloured sintered materials for each particle size and cooling rate. A high amount of CaO/SiO_2 ratios for light-coloured samples resulted in relatively low densification. The densities of light- and dark-coloured samples were in the range of 3.0 and 3.2 mg m^{-3}, respectively. It is considered that 19 min dwell time at 1700 °C was not enough to obtain a high densification rate. Therefore, sintering time (t_{dwell}) was increased from 19 to 50 min, and the effect of different cooling rates in grain growth was then investigated using a similar sintering scheme.

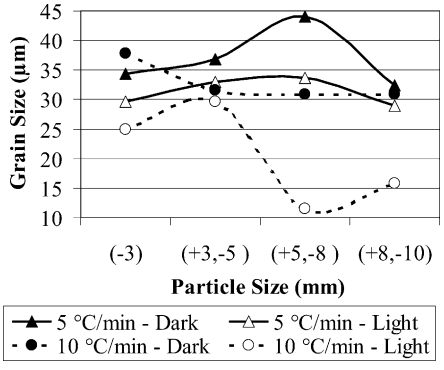

Fig. 1. MgO mean grain size as a function of particle size (T_s = 1700 °C and t_{dwell} = 19 min).

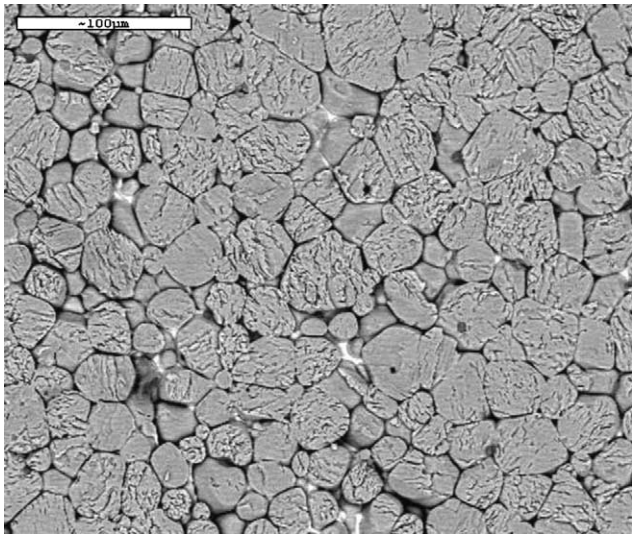

Fig. 2. SEM micrograph of sintered magnesite (+5,−8 mm dark, T_s = 1700 °C, t_{dwell} = 19 min and cooling rate = 5 °C min^{-1}).

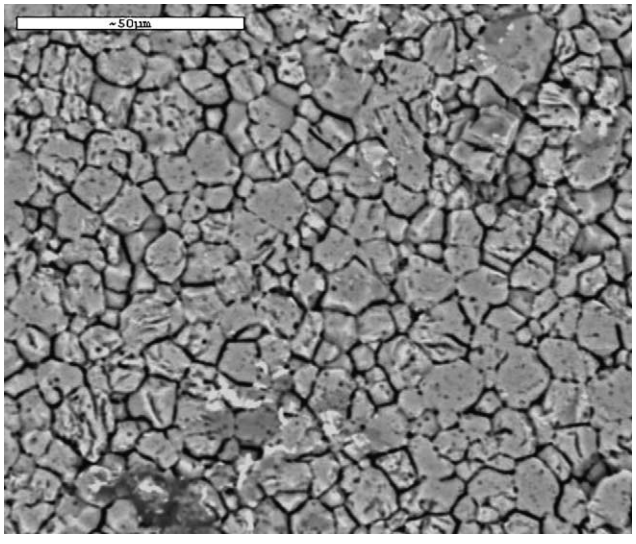

Fig. 3. SEM micrograph of sintered magnesite (+5,−8 mm light, T_s = 1700 °C, t_{dwell} = 19 min and cooling rate = 10 °C min^{-1}).

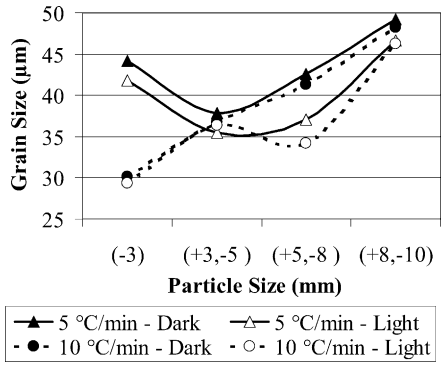

Fig. 4. MgO mean grain size as a function of particle size (T_s = 1700 °C and t_{dwell} = 50 min).

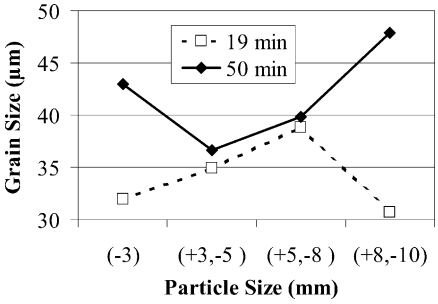

Fig. 6. The average grain size of dark and light coloured samples for each dwell time, as a function of particle size (T_s = 1700 °C and cooling rate = 5 °C min^{-1}).

Fig. 4 illustrates that the increase in the dwell time resulted in a considerable enlargement in MgO mean grain size for each particle size in comparison with Fig. 1. Fig. 5 shows the greatest mean grain size achieved using longer dwell time and lower cooling rate. Fig. 4 shows that the increase in each particle size in general led to a marked improvement in grain growth, but the change in the cooling rate as a function of particle size did not improve grain size significantly. The particle size of −3 mm, using cooling rate of 5 °C min^{-1}, demonstrated a different trend from the samples sintered with a cooling rate of 10 °C min^{-1}. It is known that [20,21] particle size is a densification-rate determining factor, and finer particles react faster. It is, therefore, possible that both the decline in cooling rate and the increase in dwell time, making reaction time longer, led to greater enhancement in grain size.

The average grain size values of dark and light coloured samples for both 19 and 50 min dwell time were then calculated separately based on the lowest cooling rate, which showed the greatest improvement in grain growth. The significant increase in average grain size with increasing dwell time as a function of particle size was given in Fig. 6. The improvement in grain size in terms of cooling rate was especially significant for the smallest (35%) and coarsest (>55%) particle size, though medium particles showed a similar trend to each other. It can be concluded that the rise in dwell time was a major factor affecting grain growth as a function of particle size (Fig. 6).

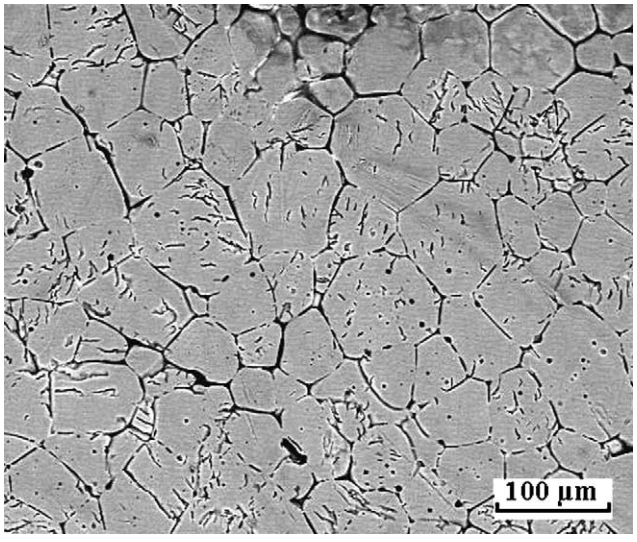

Fig. 5. SEM micrograph of sintered magnesite (+8,−10 mm dark, T_s = 1700 °C, t_{dwell} = 50 min and cooling rate = 5 °C min^{-1}).

EDX analysis of sintered magnesite samples demonstrated a similar trend for impurities as shown in Tables 1 and 2, except for CaO content. Table 2 illustrates that the amount of CaO did not show a marked change based on the cooling rate for each particle size, where the amount of CaO in dark-coloured sintered magnesites was lower than that of light-coloured samples. It is reported that [14] keeping the level of CaO low prevents the formation of low melting point calcium aluminate, which can lead to fractures and destruction of the lining, in the magnesia-based brick structure during firing. A carefully adjusted CaO content forms a protective coating in the sintering zone. In addition, a larger amount of silicate in the microstructure forms interconnected silicate networks, which can act as crack propagation paths, and decrease refractoriness and the resistance to spalling [15]. In general, the SiO_2 and Fe_2O_3 content were relatively higher, but CaO/SiO_2 ratios were predominantly lower in the dark colour samples than those of light colour materials for each particle size. Bulk density values of light and dark-coloured samples were about ~3.3 mg m^{-3}, and a high densification rate was obtained with increasing dwell time.

Furthermore, two types of sintered magnesite were used in order to investigate the effect of grain growth using a different sintering regime, but similar to industrial conditions, where each sample was sintered at ~1800 °C for 19 min, with a cooling rate of 25 °C min^{-1}. Bulk density values of all samples increased with increasing sintering temperature, and they were approximately 3.4 mg m^{-3}. The chemical composition of samples A and B for each particle size was given in Table 3. On the basis of EDX analysis, the average values of light- and dark-coloured samples including each particle size are as follows: (i) 0.89% SiO_2, 1.20% CaO, 0.41% Fe_2O_3, and CaO/SiO_2 ratio 1.35, designated as sample A, and (ii) 0.82% SiO_2, 0.72% CaO, 0.57% Fe_2O_3, and CaO/SiO_2 ratio 0.87, illustrated as sample B.

Table 3 indicates that the amount of SiO_2 in dark-coloured samples (for A and B) was higher than that of light-coloured samples. For sample A, CaO content in dark-coloured samples was higher than that of light-coloured samples; however, the amount of CaO in dark-coloured samples was generally lower than that of light-coloured sintered magnesites for sample B. EDX analysis showed that the amounts of Fe_2O_3 were $\leq$0.7 and $\leq$1.2% for samples A and B, respectively. It is known that [22] magnesia-based bricks increase coating stability and corrosion resistance by the addition of pure iron oxides, ~1%. In addition, the bricks show significant development of direct bonding by the formation of MgO–Fe_2O_3, which provides more strength at high temperatures and less deterioration due to a great diffusibility of ferric oxide [23]. On the other hand, the effect of phase changes from MgO–FeO to MgO–Fe_2O_3 on the bonded texture might be disadvantageous in developing high thermal spalling resistance with the addition of a high amount of iron oxides, >1% [16]. A reducing atmosphere accelerates the decomposition of alkaline salts, which causes their corrosive power to be increased [24]. It is reported that [25,26] when MgO–FeO is oxidised, the volumetric expansion is about 8–23%, depending on the amount of FeO. The dissolution of Fe_2O_3 in MgO leads to the formation of cation vacancies, which introduces defects in the host lattice. This condition affects the brick severely and may lead to premature wear. During ferrite formation, the reaction rate depends on temperature, grain size distribution, density and also on the partial oxygen pressure, because the concentration gradients over the reaction layer increase with decreasing partial oxygen pressure. The ferrous content of the final product depends on the homogeneity of the starting mixture. A magnesia-based brick for the cement industry should therefore have as little Fe_2O_3 as possible (preferably under 1%) [13]. Furthermore, the average value of CaO/SiO_2 ratio in sample A was found to be significantly higher than that of sample B. These ratios given in Table 3 were in general good agreement with a literature value of ~1.7–2.2, if $\sum(CaO + SiO_2) > 1.25$ [13]. It is stated that [13] much higher and lower values of CaO/SiO_2 ratios leads to abrasion and a decrease in refractoriness, and minimised CaO/SiO_2 ratio prevents the formation of low-melting compounds with brick and kiln feed components.

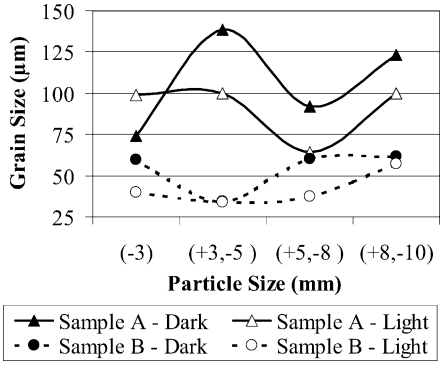

Fig. 7. MgO mean grain size as a function of particle size (T_s = 1800 °C, t_{dwell} = 19 min and cooling rate = 25 °C min^{-1}).

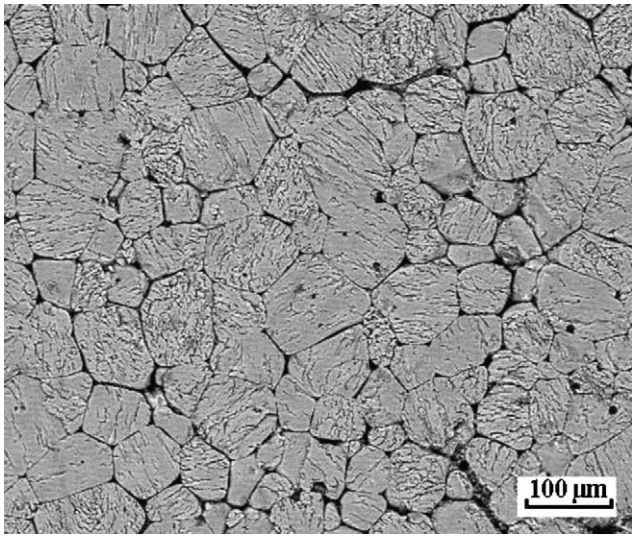

Fig. 8. SEM micrograph of sintered magnesite (sample B: +8,−10 mm dark, T_s = 1800 °C, t_{dwell} = 19 min and cooling rate = 25 °C min^{-1}).

Fig. 7 shows that there was in general a marked improvement in grain size with increasing sintering temperature for samples A and B, in comparison with Figs. 1 and 4. The grain size of dark-coloured samples was considerably higher than that of light-coloured samples (Fig. 7). Fig. 8 illustrates that the most favourable grain growth (~62 μm) was obtained from +8,−10 mm particle size for sample B, with a CaO/SiO_2 ratio of ~0.9. The +3,−5 mm particle size was found to be an optimum range to attain maximum grain size (~140 μm) in the dark-coloured samples 'A' (Fig. 9), where the average CaO/SiO_2 ratio is about ~1.4. There was a marked improvement in mean grain size of sample A, as compared to sample B, by a factor of 2.3. It is considered that the rise in the sintering temperature and chemical purity

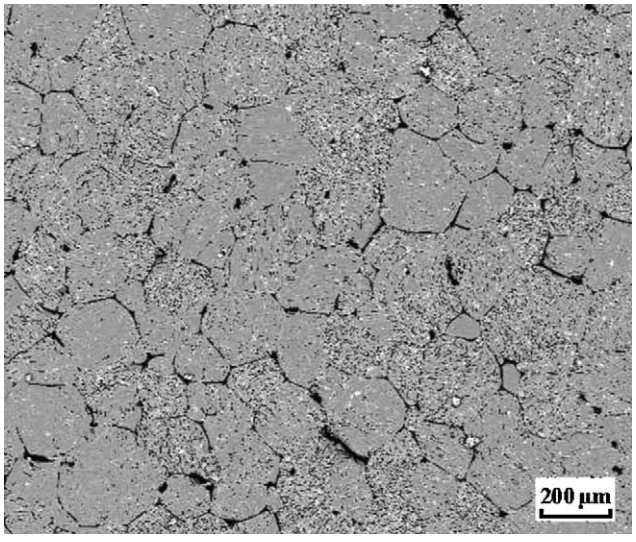

Fig. 9. SEM micrograph of sintered magnesite (sample A: +3,−5 mm dark, T_s = 1800 °C, t_{dwell} = 19 min and cooling rate = 25 °C min^{-1}).

with the optimum CaO/SiO_2 ratio were found to be major important parameters affecting grain growth of sintered magnesites markedly.

4. Conclusions

For the samples sintered at 1700 °C for 19 min, the lowest cooling rate (5 °C min^{-1}) led to a significant improvement in grain growth. Furthermore, the increased dwell time up to 50 min resulted in a marked enlargement in mean grain size, but reduced the effect of cooling rate considerably. In addition, the rise in the sintering temperature up to ~1800 °C improved the densification and gave rise to maximum enhancement in grain size. Sample A with a relatively low Fe_2O_3 content and high CaO/SiO_2 ratio showed the greatest development in grain size in comparison with sample B. In general, dark-coloured samples with a high amount of SiO_2 content illustrated a significant increase in grain growth as compared to light-coloured samples, which consist of relatively high CaO/SiO_2 ratios. Dark-coloured sample A, sintered at 1800 °C, with a +3,−5 mm particle range showed a maximum grain growth. There was a marked fluctuation in grain size of sintered magnesite samples as a function of particle size, and thus the change in particle size used in this work was not entirely an effective parameter to increase grain size. The lowest cooling rate, the longest dwell time and the increased sintering temperature, with optimum CaO/SiO_2 ratio, were subsequently found to be major parameters improving grain growth of magnesites substantially.

Acknowledgements

This work was supported by the ''TÜBİTAK Ceramic Research Centre'' (Project no.: P/99-09). KÜMAŞ (Kütahya Magnesite Corporation) is thanked for supplies of sintered magnesite. The helpful discussion of Dr. F. Kara is also gratefully acknowledged.

References

[1] W.D. Kingery, Structure and Properties of MgO and Al_2O_3 Ceramics, Advances in Ceramics, vol. 10, The American Ceramic Society, Inc., Massachusetts Institute of Technology, Cambridge, USA, 1984.
[2] K. Itatani, M. Nomura, A. Kishioka, M. Kinoshita, Sinterability of various high-purity magnesium oxide powders, J. Mater. Sci. 21 (1986) 1429–1435.
[3] R.W. Rice, Strength/grain-size effects in ceramics, Proc. Br. Ceram. Soc. 20 (1972) 205–257.
[4] R.W. Rice, Strength and fracture of hot-pressed MgO, Proc. Br. Ceram. Soc. 20 (1972) 329–363.
[5] C. Aksel, B. Rand, F.L. Riley, P.D. Warren, Mechanical properties of magnesia–spinel composites, J. Eur. Ceram. Soc. 22 (5) (2002) 745–754.
[6] C. Aksel, P.D. Warren, Work of fracture and fracture surface energy of magnesia–spinel composites, Compos. Sci. Technol. 63 (10) (2003) 1433–1440.
[7] C. Aksel, F.L. Riley, Effect of particle size distribution of spinel on the mechanical properties and thermal shock performance of MgO–spinel composites, J. Eur. Ceram. Soc. 23 (16) (2003) 3079–3087.
[8] C. Aksel, Thermal shock behaviour and mechanical properties of magnesia–spinel composites, Ph.D. Thesis, Department of Materials Engineering, University of Leeds, UK, 1998.
[9] W.E. Lee, W.M. Rainforth, Ceramic Microstructures Property Control by Processing, Chapman & Hall, UK, 1994.
[10] P. Williams, D. Taylor, J.S. Soady, in: Proceedings of Conference on Refractories for the Steel Industry, Commission of European Community, Elsevier, 1990.
[11] P. Marechal, Thermal shock resistance of electrofused magnesia grains, Bull. Am. Ceram. Soc. 70 (11) (1991) 1780–1782.
[12] Refractories Handbook, The Technical Association of Refractories, Tokyo, Japan (a founding member of UNITECR), 1998.
[13] H.J. Klischat, P. Bartha, Further development of magnesia spinel bricks with their own specific properties for lining the transition and sintering zones of rotary cement kilns, World Cement (September 1992) 52–58.
[14] H.K.F. Harburg, Experience with magnesium–aluminium–spinel bricks in a 3000 t/d rotary kiln, Zement-Kalk-Gibs Int. 3/4 (1993) 446–454.
[15] R.M. Evans, Magnesia–alumina spinel raw materials production and preparation, Am. Ceram. Soc. Bull. 72 (4) (1993) 59–63.
[16] A. Sato, I. Tsuchiya, H. Takahashi, T. Ishii, K. Takebayashi, T. Kawakami, Effect of thermal shock on the structural changes of the basic refractories for cement rotary kiln, Taikabutsu Overseas 8 (1) (1986) 37–39.
[17] BS 7134, Methods for determination of density and porosity, British Standard Testing of Engineering Ceramics, Part 1, Section 1.2, 1989.
[18] D.J. Clinton, in: R. Freer (Ed.), A Guide to Polishing and Etching of Technical and Engineering Ceramics, The Institute of Ceramics, Middlesex, UK, 1987.
[19] M.I. Mendelson, Average grain size in polycrystalline ceramics, J. Am. Ceram. Soc. 52 (1969) 443–446.
[20] S.F. Hulbert, Models for solid state reactions in powdered compacts, Br. Ceram. Soc. (1968) 1–32.
[21] J.H. Taplin, Index of reaction—a unifying concept for the reaction kinetics of powders, J. Am. Ceram. Soc. 57 (3) (1974) 140–143.
[22] M. Olbrich, F. Dobrowsky, Periclase spinel bricks in the cement industry, Radex-Rundschau 2/3 (1990) 300–311.
[23] J. Mosser, G. Buchebner, K. Dosinger, New high-quality MgO–Cr_2O_3-bricks and Cr-free alternatives for the lining of RH/DH-vessels, Veitsch-Radex Rundschau 1 (1997) 11–23.
[24] K. Hara, H. Kusunose, I. Kenmochi, K. Tokunaga, Study for improvement of spinel bricks, Taikabutsu Overseas 8 (1) (1986) 31–32.
[25] P. Reijnen, The Formation of Ferrites from the Metal Oxides, in: G.H. Stewart (Ed.), Science of Ceramics, vol. 3, Academic Press, London, New York, 1967, pp. 245–261.
[26] S.F. Hulbert, H.H. Wilson, D.A. Venkatu, Kinetics of the reaction between MgO and Fe_2O_3 in powder compacts, Trans. J. Br. Ceram. Soc. 69 (1970) 9–13.